Experimental and Numerical Study on Laminar Flame Characteristics of Methane Oxy-fuel Mixtures Highly Diluted with CO 2

ARTICLE *in* ENERGY & FUELS · OCTOBER 2013

Impact Factor: 2.79 · DOI: 10.1021/ef401220h

6 AUTHORS, INCLUDING:

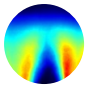

Yongliang Xie
Xi'an Jiaotong University
10 PUBLICATIONS **47** CITATIONS
SEE PROFILE

Jinhua Wang
Xi'an Jiaotong University
33 PUBLICATIONS **568** CITATIONS
SEE PROFILE

Zhang Meng
Xi'an Jiaotong University
17 PUBLICATIONS **52** CITATIONS
SEE PROFILE

Zuohua Huang
Xi'an Jiaotong University
423 PUBLICATIONS **5,215** CITATIONS
SEE PROFILE

energy&fuels

Article

pubs.acs.org/EF

Experimental and Numerical Study on Laminar Flame Characteristics of Methane Oxy-fuel Mixtures Highly Diluted with CO_2

Yongliang Xie, Jinhua Wang,* Meng Zhang, Jing Gong, Wu Jin, and Zuohua Huang*

State Key Laboratory of Multiphase Flow in Power Engineering, Xi'an Jiaotong University, Xi'an, Shaanxi 710049, People's Republic of China

ABSTRACT: An experimental and numerical study on laminar flame characteristics of methane oxy-fuel mixtures highly diluted with CO_2 was conducted using a constant volume chamber and CHEMKIN package. The effects of high CO_2 dilution on combustion chemical reaction, flame instability, and flame radiation of $CH_4/CO_2/O_2$ mixtures were studied. The laminar burning velocities of $CH_4/CO_2/O_2$ mixtures decrease with the increase of the CO_2 fraction. CO_2 directly participates in the chemical reaction through the elementary reaction OH + CO = H + CO_2 and inhibits the combustion process by the competition of the H radical between the reverse reaction of OH + CO = H + CO_2 and the reaction H + O_2 = O + OH. This effect is more obvious for highly diluted CO_2 in the case of $CH_4/CO_2/O_2$ mixtures. CO_2 suppresses the flame instability by the combined effect of hydrodynamic and thermal-diffusive instabilities. The radiation of CH_4 oxy-fuel combustion is much stronger than that of CH_4/air combustion mainly because of the existence of a large fraction of CO_2 in $CH_4/CO_2/O_2$ flames, which will influence the wall temperature and temperature distribution in the gas turbine combustor.

1. INTRODUCTION

With an increasing concern on global warming, the studies on the reduction of greenhouse gas emissions, with the dominant contributor being CO_2, have attracted increasing attention in recent years. Although renewable energy sources, such as solar energy, can be used to control CO_2 emissions, it is still a long way for them to meet the incredible amount of energy demand. The major energy sources now are still fossil fuel, which inevitably produces CO_2 when burned. To solve the problem, carbon capture and storage (CCS) is being widely studied.[1,2] CCS contains a wide range of technologies that allow CO_2 emissions from fossil fuel combustion to be transported to safe geological storage rather than be released into the atmosphere. The oxy-fuel combustion which burns the fuel in oxygen with dilution rather than air is one of the most promising technologies for CCS. Recycled flue gas (mainly CO_2 and H_2O) is generally needed for temperature control and material safety consideration. With pure oxygen as the oxidizer, the NO_x problem during the combustion process may be solved and the CO_2 concentration in the exhaust gas is high and much suitable for CCS.[3]

Natural gas, with the main composition of CH_4, is a clean fuel for power generation. In combination with CCS, methane oxy-fuel combustion can achieve zero emissions, including CO_2. To understand the behavior of oxy-fuel flames better and apply it to industrial facilities, the fundamental data are required, such as laminar burning velocity, which is a fundamental parameter of the mixture, and it is the basis of the investigations on flame properties, such as flame stability, extinction, and flashback. Moreover, it can also be used to validate and revise the chemical reaction mechanisms and play an important role in the design and optimization of combustion equipments, such as internal combustion engines and power plant burners. Laminar burning velocities have been extensively studied for methane.[4,5] However, these previous studies were conducted on the CH_4/air mixtures, and few studies were reported on the CH_4 oxy-fuel mixtures. Meanwhile, the recent oxy-fuel combustion studies mainly focus on the solid fuel[3,6] and system analysis.[7] The investigations on fundamental characteristics of the oxy-fuel flame are still insufficient. Liu et al.[8] investigated the chemical effect of CO_2 replacement of N_2 in air on the burning velocity of CH_4 and H_2 premixed flames. It showed that the substitution of N_2 with CO_2 in the oxidizer would decrease the burning velocity. This phenomenon has been explained by the following three aspects: (1) variation of thermal and transport properties, (2) enhanced radiation of CO_2, and (3) direct chemical effects of CO_2. Wang et al.[9] studied laminar burning velocities and flame characteristics of the syngas oxy-fuel combustion and confirmed that CO_2 is directly involved in the combustion process and behaves as an inhibitor in the combustion process. Heil et al.[10] and Glarborg et al.[11] experimentally investigated the effect of CO_2 and O_2 on the burning rates of methane oxy-fuel combustion. It showed that the chemical effects of CO_2 existence have a significant influence on the production and consumption rates of CO in the oxy-fuel combustion. Moreover, although CO_2 effects have been widely investigated in CH_4 combustion, the CO_2 dilution ratio in the previous studies was still low and the highly diluted effect of CO_2 on CH_4 oxy-fuel mixtures is still far from being well-investigated.

The main objective of this study is to provide the laminar burning velocity data of $CH_4/CO_2/O_2$ mixtures at various CO_2 fractions, equivalence ratios, and pressures. Thermal and chemical effects of highly diluted CO_2 on laminar burning velocities are discussed. Moreover, flame intrinsic instability and flame radiation characteristics are also analyzed.

Received: June 29, 2013
Revised: September 18, 2013
Published: September 18, 2013

   dx.doi.org/10.1021/ef401220h | *Energy Fuels* 2013, 27, 6231−6237

2. EXPERIMENTAL SECTION

A detailed description of the experimental apparatus used in the study has been described elsewhere,[12] and a brief description is given. It consists of a constant volume combustion chamber, heating system, ignition electrodes, high-speed schlieren photography, and data acquisition system. The combustion chamber is a cylinder type with inner diameter of 180 mm, inner length of 210 mm, and volume of 5.57 L. Two quartz windows with a diameter of 80 mm are separately located on the two sides of the vessel for optical access. The centrally located electrodes are used to ignite the combustible mixture. The pressure transmitter, thermocouple, pressure transducer, and inlet and outlet valves are mounted on the chamber body. Flame propagation images are recorded by a high-speed camera (REDLAKE HG-100) operating at 10 000 frames/s with the schlieren technique.

Laminar burning velocities were measured using the outwardly spherical propagating flame method. For an outwardly spherical propagating flame, the stretched flame velocity, S_n, which reflects the flame propagation speed relative to the chamber wall, is derived from the flame radius versus time[13]

$$S_n = \frac{dr_u}{dt} \tag{1}$$

where r_u is the radius of the spherical flame and t represents the time from the spark ignition timing.

For the outwardly propagating spherical flame, the flame stretch rate, α, can be derived in the following form:

$$\alpha = \frac{d(\ln A)}{dt} = \frac{1}{A}\frac{dA}{dt} = \frac{2}{r_u}\frac{dr_u}{dt} = \frac{2}{r_u}S_n \tag{2}$$

For moderate stretch rates, the flame speed and flame stretch rate could be considered to have a linear correlation[13,14]

$$S_b - S_n = L_b\alpha \tag{3}$$

where S_b is the unstretched flame propagation speed and can be obtained as the intercept value at $\alpha = 0$ in the plot of S_n against α. The negative value of the slope of the S_n–α curve is defined as burnt gas Markstein length L_b. Then, the laminar burning velocity S_L can be obtained from the following continuity equation:

$$\rho_u S_L = \rho_b S_b \tag{4}$$

where ρ_u and ρ_b are the densities of the unburned and burned mixtures, respectively.

Usually, flame images with the radius between 5 and 25 mm are used to calculate the laminar burning velocities by considering the effect of the ignition energy and pressure rise in the combustion chamber. A flame radius less than 5 mm was not used to avoid the effect of ignition. Moreover, it should be noted that the minimum radius chosen for calculation must satisfy the condition $\delta_D/r_f \ll 1$,[15] where δ_D is the characteristic flame thickness. On the other hand, the pressure in the combustion chamber remained almost unchanged when the flame radius was smaller than 25 mm; thus, the flame propagation process can be regarded as a constant pressure process.

In this experiment, the initial pressures are set as 0.1, 0.2, and 0.3 MPa, the temperature is 300 ± 3 K, and the equivalence ratios are from 0.4 to 1.6. The CO_2 fraction in the oxidizer, ZCO_2, which is defined as $ZCO_2 = XCO_2/(XCO_2 + XO_2)$, ranges from 0.4 to 0.7. Here, X refers to the mole fraction of the specific species.

A numerical simulation of a one-dimensional, adiabatic, laminar premixed flame was conducted with the premixed code[16] of the CHEMKIN-II database[17] with a mechanism of GRI 3.0.[18] Besides the adiabatic flame, flame radiation is also calculated using an optically thin model (OTM model) with a Planck mean absorption coefficient. Even though radiation reabsorption has a great impact on the laminar flame at a very high CO_2 concentration and ultralean conditions,[19] the main objective of the present study is to compare the radiation characteristic of the $CH_4/CO_2/O_2$ flame to the traditional CH_4/air flame, which will affect the combustor wall temperature. The simple OTM model is accurate enough to show the different trends of the flame radiation and is suitable for computational fluid dynamics (CFD). GRI 1.2[20] was used to calculate the flame radiation because the calculation domain is too big to use a larger mechanism. The flame radiation is calculated by adding the radiation energy to the energy equation of PREMIX as a source term

$$\dot{m}\frac{dT}{dx} - \frac{1}{c_p}\frac{d}{dx}\left(\lambda\frac{dT}{dx}\right) + \frac{1}{c_p}\sum_{k=1}^{K}\rho Y_k V_k c_{pk}\frac{dT}{dx} + \frac{1}{c_p}\sum_{k=1}^{K}\dot{\omega}_k h_k w_k - \dot{q} = 0 \tag{5}$$

where $\dot{m}$ is the mass burning rate, x is the spatial coordinate, λ is the thermal conductivity, c_p is the heat capacity at constant pressure, ρ is the mass density, Y_k is the mass fraction of kth species, T is the local temperature, k is the total number of species, and $\dot{\omega}_k$, h_k, and w_k are the production rate, enthalpy, and molecular weight of kth species, respectively. $\dot{q}$ is the flame radiation heat flux and calculated using the OTM model

$$\dot{q} = -4\sigma K_p(T^4 - T_\infty{}^4) \tag{6}$$

$$K_p = \sum_{i=1}^{4} P_i K_i \quad i = CO_2,\ H_2O,\ CH_4, \text{ and } CO \tag{7}$$

where $\sigma = 5.669 \times 10^{-8}$ W m^{-2} K^{-4} is the Stefan–Boltzmann constant, K_i is the Planck mean absorption coefficient, P_i is the local partial pressure of the specific species, and T and T_∞ are the local and ambient temperatures, respectively.

Total radiation heat loss Q_{rad} and normalized radiation fraction X_{rad} are defined as

$$Q_{rad} = \int_0^x \dot{q}dx \tag{8}$$

$$X_{rad} = Q_{rad}/Q_{mix} \tag{9}$$

where Q_{mix} is the total lower heating value of the reactant mixtures. The calculation domain is 300 cm when considering the flame radiation and 10 cm in the case of the adiabatic flame.

3. RESULTS AND DISCUSSION

3.1. Laminar Burning Velocities of $CH_4/CO_2/O_2$ Mixtures. Figure 1 shows both the measured and calculated laminar burning velocities of $CH_4/CO_2/O_2$ mixtures versus equivalence ratio at different CO_2 fractions. Laminar burning velocities of $CH_4/CO_2/O_2$ mixtures increase with the increase of the equivalence ratio for the fuel-lean mixtures and then decrease for fuel-rich mixtures. Obviously, the laminar burning velocities decrease with the increase of the CO_2 fraction, Z, in the oxidizer. It is reasonable that the dilution effect of CO_2 decreases the flame temperature and reduces the rate of reaction and burning velocities.[21] In general, the calculated data show a reasonable agreement with the experimental data, especially for the atmospheric pressure. However, there exists a large discrepancy when the pressure is increased. The GRI 3.0 mechanism underpredicates the laminar burning velocities of CH_4 oxy-fuel combustion. The discrepancy becomes larger with the decrease of the CO_2 fraction. This may be due to the large dissociation of CO_2 for $CH_4/CO_2/O_2$ mixtures because the adiabatic temperature is high when the CO_2 fraction is lower. Carbon–oxygen double bonds in CO_2 are very strong, and it will take a high temperature to break them. When the CO_2 fraction is 0.4, the adiabatic flame temperature is over 2500 K. Thermal dissociation of CO_2 may occur at such a high temperature.[11] In addition, radiation reabsorption that occurs in practical flames has a positive effect on the laminar burning velocities[22] when the CO_2 fraction is high in the mixture. Therefore, it is reasonable that the experimental values are

dx.doi.org/10.1021/ef401220h | Energy Fuels 2013, 27, 6231–6237

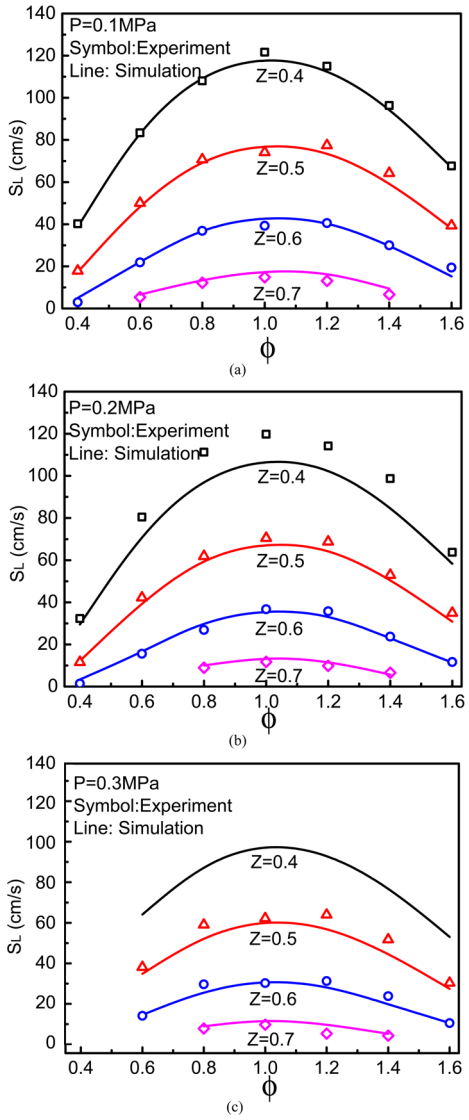

Figure 1. Laminar burning velocities of the $CH_4/CO_2/O_2$ mixture: (a) 0.1 MPa, (b) 0.2 MPa, and (c) 0.3 MPa.

larger than the calculated values. Moreover, the laminar burning velocities measured in experiments are lower than those predicated by simulation for an ultralean mixture as Z = 0.7 and φ = 0.4. This may be due to the fact that the spherical laminar flame is strongly affected by radiation when the laminar flame speed is low (below 15 cm/s), and those experimental results will be influenced by the radiation-inducted flow effect and, hence, lower than the true value.[23] On the whole, the GRI 3.0 mechanism needs to be revised and validated for the calculation of CH_4 oxy-fuel mixtures when the participation of CO_2 to the chemical reaction is considered, especially for the lower CO_2 dilution with a high adiabatic flame temperature.

3.2. Thermal and Chemical Effect of Highly Diluted CO_2 on $CH_4/CO_2/O_2$ Mixtures. Figure 2 shows the adiabatic flame temperature of the $CH_4/CO_2/O_2$ mixture at different equivalence ratios. Usually, the elementary reactions are greatly influenced by the adiabatic flame temperature (T_{ad}), and the different T_{ad} corresponds to different reaction rate constants. Thus, the adiabatic flame temperature is often used as an indicator to investigate the laminar flame. Previous research[5] showed that the thermal effect of CO_2 can be studied by the

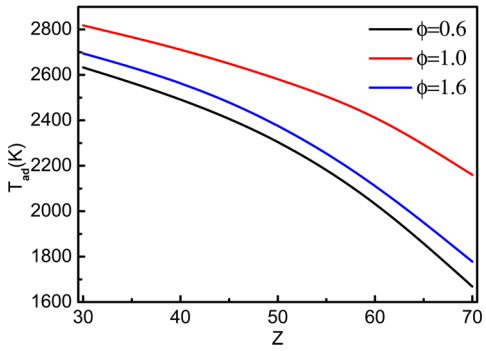

Figure 2. Adiabatic flame temperature of the mixture for different equvalence ratios (P = 0.1 MPa).

investigation of the adiabatic flame temperature, and this effect has great influence on the laminar burning velocities. It can be seen that the adiabatic flame temperature decreases with the addition of CO_2 in the mixture for all equivalence ratios. However, it should be noted that the adiabatic flame temperature does not decrease linearly with the increase of the CO_2 fraction. For a mixture with a higher CO_2 fraction, CO_2 has a stronger thermal effect. Meanwhile, the mixture at lean or rich conditions shows a stronger thermal effect than that at stoichiometric conditions.

Figure 3 gives the sensitivity coefficients of the laminar burning velocity for the $CH_4/CO_2/O_2$ flames at various CO_2

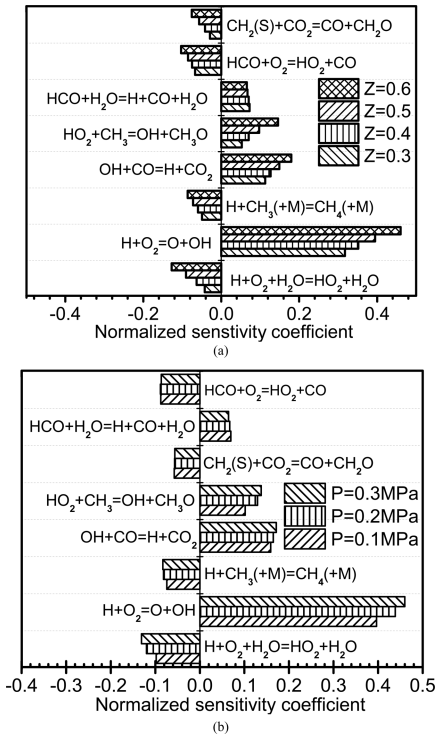

Figure 3. Sensitivity coefficient to laminar burning velocities (ϕ = 0.6): (a) P = 0.1 MPa and (b) Z = 0.5.

fractions and pressures. It is obvious that the CO_2 fraction and pressure both affect the sensitivity coefficients. With the increase of the CO_2 fraction in the mixture, sensitivity coefficients of the majority of elementary reactions all increase. The sensitivity coefficient of the chain-branching reaction H + O_2 = O + OH increases with the increase of the pressure.

dx.doi.org/10.1021/ef401220h | Energy Fuels 2013, 27, 6231−6237

Westbrook et al.[24] reported that the chain-branching reaction H + O_2 = O + OH has the largest positive sensitivity factor for hydrocarbon/air flames. Similar to hydrocarbon/air flames, elementary reaction H + O_2 = O + OH also has the largest positive sensitivity coefficient for the $CH_4/CO_2/O_2$ mixtures, and its coefficient is much higher than those of other elementary reactions. Elementary reaction OH + CO = H + CO_2 has the second highest positive sensitivity coefficient. The reverse of this reaction was thought as the main pathway in which CO_2 participates in chemical reactions.[8,25,26] The mole fraction profiles of H, O, and OH for the $CH_4/CO_2/O_2$ mixture for various CO_2 fractions are given in Figure 4. The

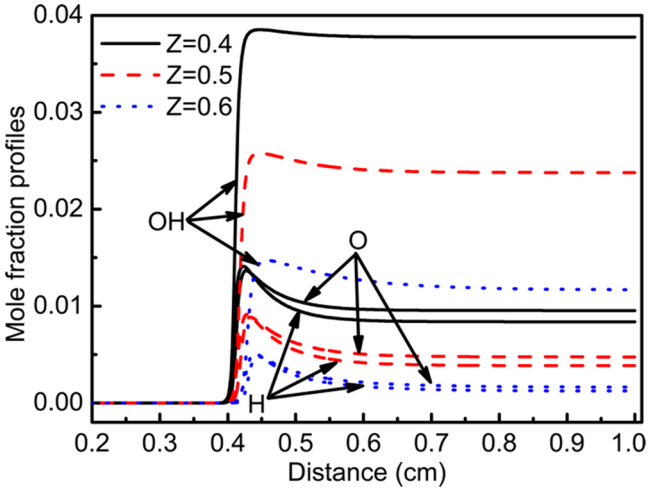

Figure 4. Mole fraction profiles of H, O, and OH radicals for the $CH_4/CO_2/O_2$ mixture at different CO_2 fractions (ϕ = 0.6 and P = 0.1 MPa).

free radicals decrease significantly with the increase of the CO_2 fraction. This leads to the reduction of the reaction rate because H, O, and OH play a crucial role in elementary reactions.[8,27] The detailed chemical effect of highly diluted CO_2 will be discussed in a later section.

The bond energy of N≡N for N_2 is 945 kJ/mol, and it is much larger than that of C═O for CO_2 (531 kJ/mol). This indicates that CO_2 tends to participate in the combustion reaction compared to N_2. Previous studies indicated that the most important reaction associated with the direct chemical participation of CO_2 in hydrocarbon combustion diluted with CO_2 is OH + CO = H + CO_2. The effect of CO_2 on the combustion reaction is studied here by the comparison between the calculation of the flames using CO_2 and that using FCO_2 (fictitious CO_2),[8] which possesses identical thermal and transport properties. Moreover, FCO_2 does not directly participate in any chemical reaction but acts as a third body and is assigned the same third-body collision efficiency as CO_2.[8,9] Figures 5−7 give the mole fractions of CO and CO_2, mole fractions of key intermediate radicals, and production rate of key elementary reactions, respectively. The flame temperature, mole fraction of intermediate radicals, and production rate of elementary reactions all decrease when the chemical effect of CO_2 is considered. Besides, the mole fraction of CO_2 decreases but that of CO increases when CO_2 participates in the chemical reactions. The difference between CO_2 and FCO_2 proves that CO_2 indeed has a great influence on the chemical reaction by directly participating in the reaction because CO_2 and FCO_2 have the same thermal and transport properties. In

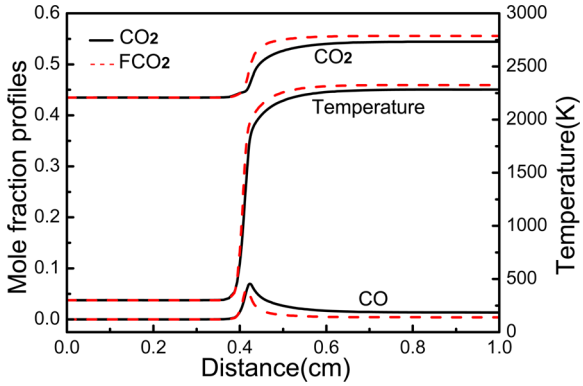

Figure 5. Mole fractions of CO and CO_2 and temperature profiles for $CH_4/CO_2/O_2$ and $CH_4/FCO_2/O_2$ mixtures (ϕ = 0.6, Z = 0.5, and P = 0.1 MPa).

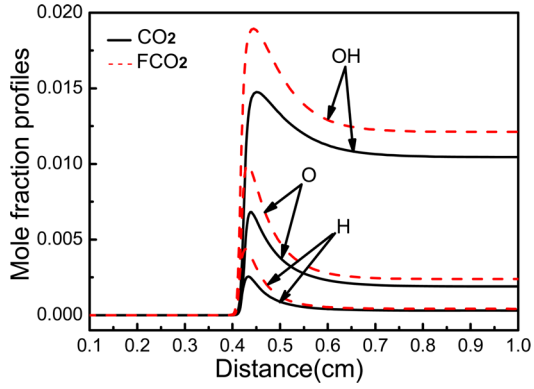

Figure 6. Mole fraction profiles of H, O, and OH radicals for the $CH_4/CO_2/O_2$ mixture (ϕ = 0.6, Z = 0.5, and P = 0.1 MPa).

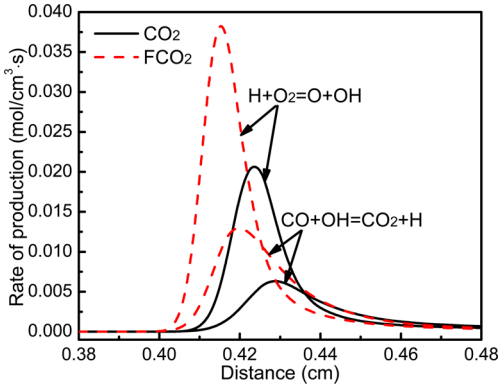

Figure 7. Rate of production of important elementary reactions for the $CH_4/CO_2/O_2$ mixture (ϕ = 0.6, Z = 0.5, and P = 0.1 MPa).

terms of elementary reactions, the direct chemical participation of CO_2 causes OH + CO = H + CO_2 to react in the opposite direction and significantly consume the H radical. Thus, the reaction H + O_2 = O + OH is suppressed. This means that, because of the existence of a large fraction of CO_2, the competition for the H radical between the reverse reaction of OH + CO = H + CO_2 and the most sensitive elementary reaction H + O_2 = O + OH significantly reduces the reaction rate of combustion. This is different from the traditional CH_4/air combustion diluted with exhaust gas recirculation (EGR), which has a lower CO_2 dilution and just reduces the reaction rate slightly.[28]

dx.doi.org/10.1021/ef401220h | Energy Fuels 2013, 27, 6231−6237

3.3. Effect of Highly Diluted CO_2 on Flame Intrinsic Instability. There are three mechanisms of flame intrinsic instabilities, the hydrodynamic instability, the diffusive-thermal instability, and buoyancy-driven instability.[27] The buoyancy-driven instability can be neglected in this study because the flame-propagating speed is relatively high. The hydrodynamic instability is caused by gas thermal expansion across the flame front and is characterized by the thermal expansion ratio and flame thickness.[29] Essentially, the hydrodynamic instability always exists. In general, a decrease in flame thickness and an increase in the thermal expansion ratio will enhance the hydrodynamic instability. Diffusive-thermal instability is resulting from non-equal diffusion between heat and mass and can be assessed by the Lewis number, which is defined as the ratio of mixture thermal diffusivity and mass diffusivity.[30] Yu et al.[31] studied the flame instability of CH_4 oxy-fuel combustion with a flat-flame burner, and this study presents the intrinsic flame instability of the stretched spherical flame. The instability parameters and flame images at different CO_2 fractions are given in Figure 8. Those parameters are the density ratio of

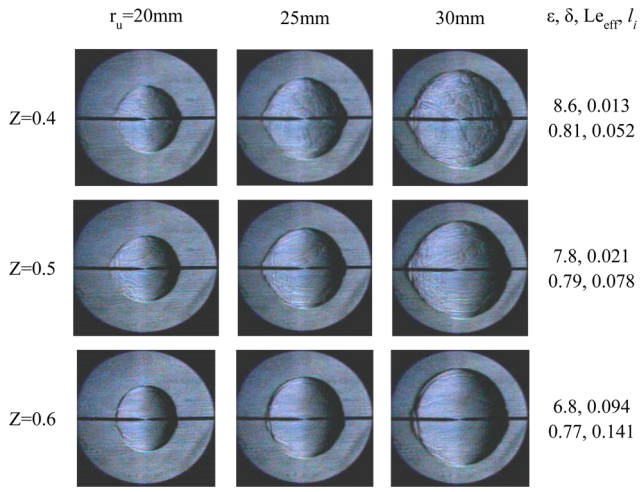

Figure 8. Flame images and instability parameters at various CO_2 fractions [ϕ = 0.6, P = 0.2 MPa, δ, and l_i (mm)].

unburned mixtures to burned mixtures, ε, flame thickness, δ, effective Lewis number, Le_{eff}, and flame intrinsic instability scale, l_i. Among them, the effective Lewis number is determined using the formula

$$1/Le_{eff} = (X_1/Le_1 + X_2/Le_2 + ... + X_i/Le_i) / (X_1 + X_2 + ... + X_i) \quad (10)$$

The effective Lewis number takes into account the thermal and mass diffusivities of the insufficient species. Thus, for the present lean $CH_4/CO_2/O_2$ mixtures, the considered species are CH_4 and O_2.

The intrinsic flame instability scale is the characteristic scale of hydrodynamics combined with diffusive-thermal effects. It is calculated from the equation

$$l_i = \pi/k_{\sigma_{max}} \quad (11)$$

where σ represents the growth rate of flame front disturbances and is calculated using the formulation by Yuan et al.,[32] in which the high-order temperature relaxation term is added to the original Sivashinsky's formulation.[30] In the case of a Lewis number less than unity, σ is estimated as

$$\sigma = \Omega_0 S_L k - \Omega_1 \alpha k^2 - 4\alpha\delta^2 k^4 \quad (12)$$

where k is wavenumber of the disturbance, $k_{\sigma_{max}}$ is the wavenumber corresponding to the maximum growth rate. The first term on the right-hand side represents the hydrodynamic instability; the second term represents the diffusive-thermal instability; and the third term represents the high-order temperature relaxation term proposed by Yuan et al.[32]

As shown in Figure 8, the flame front presents the cellular structure and some cracks at Z = 0.4. With the increase of the CO_2 fraction, the cellular structure is decreased and the flame front becomes smooth. The density ratio is decreased with the increase of the CO_2 fraction, and this reflects the decrease of hydrodynamic instability. The flame thickness increases with the increase of the CO_2 fraction, and this also suppresses the hydrodynamic instability. The effective Lewis number is less than unity and decreases with the increase of the CO_2 fraction, and this promotes the diffusive-thermal instability. Meanwhile, the flame intrinsic instability scale, l_i, increases with the increase of the CO_2 fraction, and this indicates that the existence of CO_2 will suppress the flame instability because of the combined effects of hydrodynamic and diffusive-thermal instabilities.

3.4. Effect of Highly Diluted CO_2 on Flame Radiation Characteristics. Flame radiation is a very important parameter for the investigation of the flame characteristics and the design of the combustor.[33] Ju et al.[34] studied the effects of the Lewis number and radiation heat loss on bifurcation and extinction of the flame. They found that the interaction between the Lewis number and radiation heat loss dramatically affects flame bifurcation and extinction. Kadowaki[35] found that heat loss had a great influence on the unstable behavior of cellular flames for the sub-unity Lewis number mixtures. Flame radiation will also affect the wall temperature and temperature distribution in the combustor. In comparison to the traditional CH_4/air flame, the $CH_4/CO_2/O_2$ flame may have different radiation characteristics because the absorption coefficients of N_2 and CO_2 are different. The radiation characteristics of $CH_4/CO_2/O_2$ and CH_4/air flames with the same adiabatic flame temperature are given in Figure 9, and the conditions and properties of these flames are

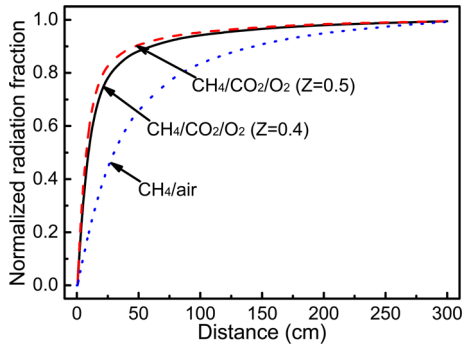

Figure 9. Comparison of the normalized radiation fraction between different flames (conditions are shown in Table 1).

given in Table 1. Obviously, the radiation of CH_4 oxy-fuel combustion is much stronger than that of CH_4/air combustion. One main reason is the large mole fraction of CO_2 in the $CH_4/CO_2/O_2$ flames, as shown in Figure 10. Planck mean absorption coefficients of CO_2, H_2O, CH_4, and CO are plotted in Figure 11. The Planck mean absorption coefficient of CO_2 is much

dx.doi.org/10.1021/ef401220h | Energy Fuels 2013, 27, 6231−6237

Table 1. Flame Properties for the Calculation of Flame Radiation (P = 0.1 MPa and T = 300 K)

mixtures	ϕ	CH_4	O_2	CO_2	N_2	T_{ad} (K)
$CH_4/CO_2/O_2$ (Z = 0.4)	0.4	0.107	0.537	0.356	0	2131
$CH_4/CO_2/O_2$ (Z = 0.5)	0.505	0.112	0.444	0.444	0	2135
CH_4/air	0.9	0.086	0.192	0	0.722	2134

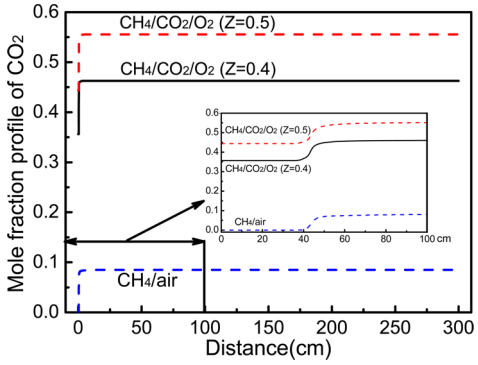

Figure 10. Comparison of the mole fraction profile of CO_2 for the flames (conditions are shown in Table 1).

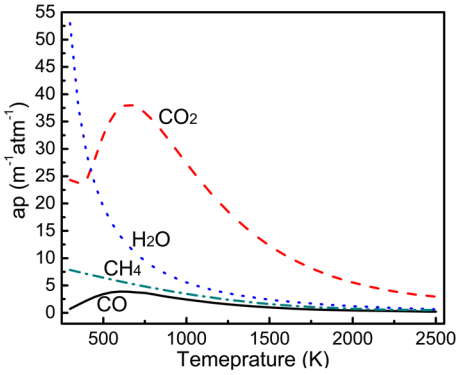

Figure 11. Temperature dependence of the Planck mean absorption coefficients for CO_2, H_2O, CH_4, and CO.

larger than those of other species in the flame temperature range. Thus, the flame radiation increases with the increase of the CO_2 fraction.

The flame radiation heat flux of different flames is given in Figure 12. The flame radiation heat flux of CH_4 oxy-fuel combustion is much larger than that of CH_4/air combustion in the region between X = 0 and 2 cm. In this region, most energy is lost by heat radiation. In this case, the intensive radiation of CH_4 oxy-fuel combustion to the combustion chamber will lead to a higher temperature in some places of the combustion chamber and may even damage the combustor. For CH_4/air combustion, the curve of flame radiation heat flux is smoother than that of CH_4 oxy-fuel combustion.

4. CONCLUSION

Laminar burning velocities of CH_4 oxy-fuel combustion were measured using an outwardly spherical propagating flame method. The effect of CO_2 on combustion chemical reactions, flame instability, and flame radiation was studied. The main results are summarized as follows: (1) Laminar burning velocities of $CH_4/CO_2/O_2$ decrease with the increase of the

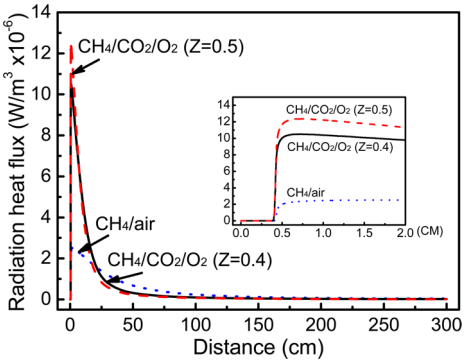

Figure 12. Radiation heat fluxes of different flames (conditions are shown in Table 1).

CO_2 fraction in the oxidizer. The methane mechanism needs to be revised for the CH_4 oxy-fuel mixtures in the case of a lower CO_2 fraction and elevated pressure, considering the participation of high CO_2 dilution on the chemical reaction. (2) CO_2 directly participates the chemical reaction through the elementary reaction OH + CO = H + CO_2 and inhibits the combustion process by the competition on the H radical between the reverse reaction of OH + CO = H + CO_2 and the reaction H + O_2 = O + OH. (3) With the increase of the CO_2 fraction, hydrodynamic instability is weakened but diffusive-thermal instability is promoted. The existence of CO_2 suppresses flame instability because of the combined effect of hydrodynamic and diffusive-thermal instabilities. (4) Radiation of CH_4 oxy-fuel combustion is much stronger than that of CH_4/air combustion because of the existence of a large fraction of CO_2 for $CH_4/CO_2/O_2$ flames, which needs to be considered in the combustor design.

AUTHOR INFORMATION

Corresponding Authors

*Fax: +86-29-82668789. E-mail: jinhuawang@mail.xjtu.edu.cn.
*Fax: +86-29-82668789. E-mail: zhhuang@mail.xjtu.edu.cn.

Notes

The authors declare no competing financial interest.

ACKNOWLEDGMENTS

This study is partially supported by the National Natural Science Foundation of China (51006080, 51376004, and 51121092). Jinhua Wang acknowledges the Japan Society for the Promotion of Science (JSPS) for a JSPS Postdoctoral Fellowship grant.

REFERENCES

(1) Park, J.; Park, J. S.; Kim, H. P.; Kim, J. S.; Kim, S. C.; Choi, J. G.; Cho, H. C.; Cho, K. W.; Park, H. S. NO emission behavior in oxy-fuel combustion recirculated with carbon dioxide. *Energy Fuels* **2007**, *21* (1), 121−129.

(2) Haszeldine, R. S. Carbon capture and storage: How green can black be? *Science* **2009**, *325* (5948), 1647−1652.

(3) Buhre, B. J. P.; Elliott, L. K.; Sheng, C. D.; Gupta, R. P.; Wall, T. F. Oxy-fuel combustion technology for coal-fired power generation. *Prog. Energy Combust. Sci.* **2005**, *31* (4), 283−307.

(4) Liao, S.; Jiang, D.; Gao, J.; Huang, Z. Measurements of Markstein numbers and laminar burning velocities for natural gas−air mixtures. *Energy Fuels* **2004**, *18* (2), 316−326.

(5) Hu, E.; Jiang, X.; Huang, Z.; Iida, N. Numerical study on the effects of diluents on the laminar burning velocity of methane−air mixtures. *Energy Fuels* **2012**, *26* (7), 4242−4252.

(6) Toftegaard, M. B.; Brix, J.; Jensen, P. A.; Glarborg, P.; Jensen, A. D. Oxy-fuel combustion of solid fuels. *Prog. Energy Combust. Sci.* **2010**, *36* (5), 581−625.
(7) Wall, T.; Liu, Y.; Spero, C.; Elliott, L.; Khare, S.; Rathnam, R.; Zeenathal, F.; Moghtaderi, B.; Buhre, B.; Sheng, C.; Gupta, R.; Yamada, T.; Makino, K.; Yu, J. An overview on oxyfuel coal combustion—State of the art research and technology development. *Chem. Eng. Res. Des.* **2009**, *87* (8), 1003−1016.
(8) Liu, F.; Guo, H.; Smallwood, G. J. The chemical effect of CO_2 replacement of N_2 in air on the burning velocity of CH_4 and H_2 premixed flames. *Combust. Flame* **2003**, *133* (4), 495−497.
(9) Wang, J.; Huang, Z.; Kobayashi, H.; Ogami, Y. Laminar burning velocities and flame characteristics of $CO-H_2-CO_2-O_2$ mixtures. *Int. J. Hydrogen Energy* **2012**, *37* (24), 19158−19167.
(10) Heil, P.; Toporov, D.; Förster, M.; Kneer, R. Experimental investigation on the effect of O_2 and CO_2 on burning rates during oxyfuel combustion of methane. *Proc. Combust. Inst.* **2011**, *33* (2), 3407−3413.
(11) Glarborg, P.; Bentzen, L. L. B. Chemical effects of a high CO_2 concentration in oxy-fuel combustion of methane. *Energy Fuels* **2007**, *22* (1), 291−296.
(12) Tang, C.; Huang, Z.; He, J.; Jin, C.; Wang, X.; Miao, H. Effects of N_2 dilution on laminar burning characteristics of propane−air premixed flames. *Energy Fuels* **2009**, *23* (1), 151−156.
(13) Bradley, D.; Gaskell, P. H.; Gu, X. J. Burning velocities, markstein lengths, and flame quenching for spherical methane-air flames: A computational study. *Combust. Flame* **1996**, *104* (1−2), 176−198.
(14) Gu, X. J.; Haq, M. Z.; Lawes, M.; Woolley, R. Laminar burning velocity and Markstein lengths of methane−air mixtures. *Combust. Flame* **2000**, *121* (1−2), 41−58.
(15) Qiao, L.; Kim, C. H.; Faeth, G. M. Suppression effects of diluents on laminar premixed hydrogen/oxygen/nitrogen flames. *Combust. Flame* **2005**, *143* (1−2), 79−96.
(16) Kee, R. J.; Grcar, J. F.; Smooke, M. D.; Miller, J. A. *PREMIX: A FORTRAN Program for Modeling Steady Laminar One-Dimensional Premixed Flames*; Sandia National Laboratories: Livermore, CA, 1998; Report SAND85-8240.
(17) Kee, R. J.; Rupley, F. M.; Miller, J. A. *Chemkin-II: A Fortran Chemical Kinetics Package for the Analysis of Gas-Phase Chemical Kinetics*; Sandia National Laboratories: Livermore, CA, 1991; Report SAND89-8009.
(18) Smith, G. P.; Golden, D. M.; Frenklach, M.; Moriarty, N. W.; Eiteneer, B.; Goldenberg, M.; Bowman, C. T.; Hanson, R. K.; Song, S.; Gardiner, W. C.; Lissianski, V. V., Jr.; Qin, Z. W. http://www.me.berkeley.edu/gri_mech/.
(19) Ruan, J.; Kobayashi, H.; Niioka, T.; Ju, Y. Combined effects of nongray radiation and pressure on premixed $CH_4/O_2/CO_2$ flames. *Combust. Flame* **2001**, *124* (1−2), 225−230.
(20) Frenklach, M.; Wang, H.; Yu, C. L.; Goldenberg, M.; Bowman, C. T.; Hanson, R. K.; Davidson, D. F.; Chang, E. J.; Smith, G. P.; Golden, D. M.; Gardiner, W. C.; Lissianski, V. http://www.me.berkeley.edu/gri_mech/.
(21) Natarajan, J.; Lieuwen, T.; Seitzman, J. Laminar flame speeds of H_2/CO mixtures: Effect of CO_2 dilution, preheat temperature, and pressure. *Combust. Flame* **2007**, *151* (1−2), 104−119.
(22) Chen, Z.; Qin, X.; Xu, B.; Ju, Y.; Liu, F. Studies of radiation absorption on flame speed and flammability limit of CO_2 diluted methane flames at elevated pressures. *Proc. Combust. Inst.* **2007**, *31* (2), 2693−2700.
(23) Chen, Z. Effects of radiation and compression on propagating spherical flames of methane/air mixtures near the lean flammability limit. *Combust. Flame* **2010**, *157* (12), 2267−2276.
(24) Westbrook, C. K.; Dryer, F. L. Chemical kinetic modeling of hydrocarbon combustion. *Prog. Energy Combust. Sci.* **1984**, *10* (1), 1−57.
(25) Glarborg, P.; Bentzen, L. L. Chemical effects of a high CO_2 concentration in oxy-fuel combustion of methane. *Energy Fuels* **2007**, *22* (1), 291−296.
(26) Mendiara, T.; Glarborg, P. Reburn chemistry in oxy-fuel combustion of methane. *Energy Fuels* **2009**, *23* (7), 3565−3572.
(27) Law, C. K. *Combustion Physics*; Cambridge University Press: Cambridge, U.K., 2006.
(28) Liu, F.; Guo, H.; Smallwood, G. J.; Gülder, Ö. L. The chemical effects of carbon dioxide as an additive in an ethylene diffusion flame: Implications for soot and NO_x formation. *Combust. Flame* **2001**, *125* (1−2), 778−787.
(29) Landau, L. On the theory of slow combustion. *Acta Physicochim. URSS* **1944**, *19*, 77−85.
(30) Sivashinsky, G. I. Instabilities, pattern formation, and turbulence in flames. *Annu. Rev. Fluid Mech.* **1983**, *15* (1), 179−199.
(31) Yu, J. F.; Yu, R.; Fan, X. Q.; Christensen, M.; Konnov, A. A.; Bai, X. S. Onset of cellular flame instability in adiabatic $CH_4/O_2/CO_2$ and CH4/air laminar premixed flames stabilized on a flat-flame burner. *Combust. Flame* **2013**, *160* (7), 1276−1286.
(32) Yuan, J.; Ju, Y.; Law, C. K. On flame-front instability at elevated pressures. *Proc. Combust. Inst.* **2007**, *31* (1), 1267−1274.
(33) Ditaranto, M.; Oppelt, T. Radiative heat flux characteristics of methane flames in oxy-fuel atmospheres. *Exp. Therm. Fluid Sci.* **2011**, *35* (7), 1343−1350.
(34) Ju, Y.; Guo, H.; Liu, F.; Maruta, K. Effects of the Lewis number and radiative heat loss on the bifurcation and extinction of CH_4/O_2-N_2−He flames. *J. Fluid Mech.* **1999**, *379*, 165−190.
(35) Kadowaki, S. The effects of heat loss on the burning velocity of cellular premixed flames generated by hydrodynamic and diffusive-thermal instabilities. *Combust. Flame* **2005**, *143* (3), 174−182.